Numerical Earthquake Response Analysis of the Earth Dams

Babak Ebrahimian [1,2], Ali Noorzad [1]

1- Faculty of Civil, Water and Environmental Engineering, Abbaspour School of Engineering, Shahid Beheshti University (SBU), Tehran, Iran

2- The Highest Prestigious Scientific and Professional National Foundation, Iran 's National Elites Foundation (INEF), Tehran, Iran

Emails: ebrahimian.babak@gmail.com; b_ebrahimian@sbu.ac.ir

Abstract

Numerical investigations are carried out to consider the seismic behavior of earth dams. A fully nonlinear dynamic finite difference analysis incorporating an elastic perfectly plastic constitutive model is taken into account to describe the stress-strain response of the soil during earthquakes. In addition, Rayleigh damping is used to increase the level of hysteretic damping in numerical analyses. The Masing rules are implemented into the constitutive relations to precisely explain the nonlinear response of soil under general cyclic loading. As a result, the soil shear stiffness and hysteretic damping can change with loading history. The constructed numerical model is comprehensive calibrated via the centrifuge test data as well as the field measurements of a real case history both in the time and frequency domains. Good agreements are shown between the computed and measured quantities. It is confirmed that the proposed numerical model can predict the essential fundamental aspects of nonlinear behavior of earth dams during earthquakes. Then, a parametric study is conducted to identify the effects of dam height and input motion characteristics on the seismic response of earth dams. To this end, three real earthquake records with different intensities and PGAs are used as the input motions.

Keywords: Numerical Modeling, Nonlinear Response, Seismic Behavior, Earth Dam.

1. INTRODUCTION

The performance of earth dams subjected to seismic actions can be evaluated through different approaches including the force-based pseudo-static methods as the simplest one, displacement-based sliding block methods and fully nonlinear dynamic analyses as the most complicated one [1,2]. The most common method named pseudo static approach is largely used in engineering practice to assess the seismic stability of earth dams. This approach is quite simple since it attempts to represent complex dynamic behavior in terms of static forces. Then, stability is expressed in terms of an overall factor of safety. However, dam response to an earthquake may be related to many factors such as dam geometry, mechanical properties of construction soils, static stresses and pore water pressures inside the dam, and input motion characteristics. Most of these factors are partially or totally neglected by the approaches traditionally adopted to assess the seismic safety of earth dams. The pseudo-static approach [3], for instance, ignores some earthquake parameters such as frequency content and duration, known to significantly influence the soil response. In fact, study of seismic response of earth dams is a complex problem that generally requires the use of dynamic methods of analysis with different levels of sophistication in terms of proper problem formulation, characterization of material properties and modeling of stress–strain soil behavior. On the other hand, numerical methods allow the most comprehensive analyses of the response of earth dams to seismic loading. Progress in the area of geotechnical computation and numerical modeling offers powerful facilities to analyze the seismic response of dams considering complex issues such as soil nonlinearity, evolution of pore pressure during dam construction and real earthquake records.

The current study paper presents numerical modeling of the seismic behavior of earth dams overlaying bedrock subjected to real earthquake records using fully nonlinear dynamic analysis approach. The effect of nonlinear soil behavior is then accounted in the analyses from the early beginning of earthquake loading. The numerical analyses are carried out using an elastic perfectly plastic soil model, capable to reproduce some basic features of cyclic soil behavior. A critical review of the role of hysteretic damping introduced by the model and the viscous damping artificially added in the analyses is addressed. First, the proposed numerical model is comprehensively calibrated against centrifuge model test data and field measurements of the Long Valley (LV) earth dam as a real case-history. In this regard, some important aspects of model calibration are discussed and emphasized. Comparison between the obtained numerical results and experimental observations shows that the current numerical procedure can accurately capture the fundamental aspects of the seismic behavior of earth

dams. Then, through a parametric study the effects of dam height and input motion characteristics are considered on the seismic response of earth dam.

2. NUMERICAL MODELING PROCEDURE

Numerical analyses are carried out using the finite difference program FLAC based on a continuum finite difference discretization using the Langrangian approach [4]. Every derivative in the set of governing equations is replaced directly by an algebraic expression written in terms of the field variables (e.g. stress or displacement) at discrete point in space. For dynamic analysis, it uses an explicit finite difference scheme to solve the full equation of motion using lumped grid point masses derived from the real density surrounding zone. The calculation sequence first invokes the equations of motion to derive new velocities and displacements from stresses and forces. Then, strain rates are derived from velocities, and new stresses from strain rates. Every cycle around the loop correspond to one time step. Each box updates all of its grid variables from known values that remain fixed over the time step being executed (Figure 1).

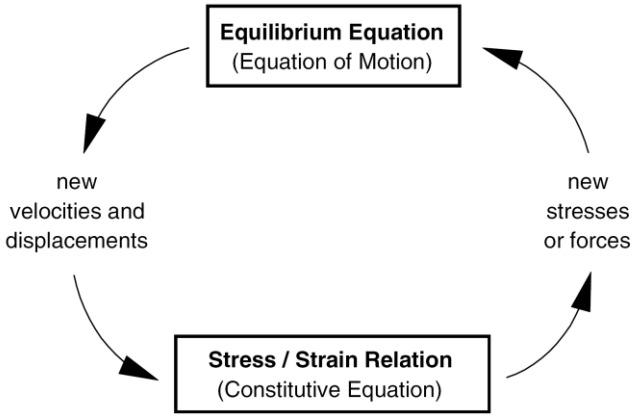

Figure 1. Basic explicit calculation cycle [4].

In simplest form, the equation of motion relates the acceleration, $d\dot{u}/dt$, of a mass, *m*, to the applied force, *F*, which may vary with time. Newton's law of motion for the mass-spring system is

$$m\left(d\dot{u}/dt\right)=F \tag{1}$$

To analyze a problem, the strain rate tensor and rotation rate tensor, having the velocity gradient, can be calculated from the following equations:

$$e_{ij}=\frac{1}{2}\left[\frac{\partial \dot{u}_i}{\partial x_j}+\frac{\partial \dot{u}_j}{\partial x_i}\right] \tag{2}$$

$$\omega_{ij}=\frac{1}{2}\left[\frac{\partial \dot{u}_i}{\partial x_j}-\frac{\partial \dot{u}_j}{\partial x_i}\right] \tag{3}$$

where, e_{ij} are the components of the strain rate and $\dot{u}_i$ are the components of the velocity. To obtain the stress tensor, the specific mechanical relationships are used which in general are as below:

$$\sigma_{ij}=M\left(\sigma_{ij},\dot{e}_{ij},\kappa\right) \tag{4}$$

where, *M* is the specific rule of behavior and *κ* is the history parameter (based on the specific rules which may or may not exist).

The selected problem is a simplified representation of a typical earth dam geometry. The dam section is a symmetric zone section with central clay core resting on bedrock as shown in Figure 2. Five earth dam cross sections with different heights i. e., *H*= 40, 80, 120, 200 and 280 *m* are analyzed in this study.

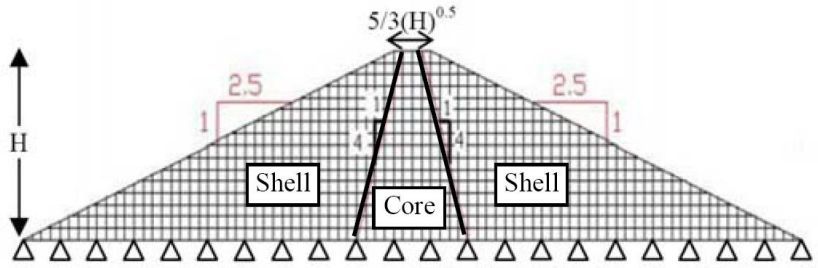

Figure 2. Geometry of dam

Mohr-Coulomb constitutive relation is used to model the soil behavior. The failure envelope for this model corresponds to a Mohr-Coulomb criterion (shear yield function) with tension cutoff (tensile yield function). The stress-strain relationship is linear elastic-perfectly plastic. The linear behavior is determined by elastic shear and bulk modules. The plastic behavior is defined by the angle of internal friction and cohesion of soil. The shear modulus of sandy soil as shell materials is calculated with the formula given [5]:

$$G_{\max} = 8400\frac{(2.17-e)^2}{1+e}\left(\sigma_0'\right)^{0.6} \tag{5}$$

where, G_{max} is the maximum (small strain) shear modulus in kPa, e is the void ratio and σ_m' is the mean effective confining stress in kPa. The Poisson's ratio for shell materials is taken as 0.3.
The shear modulus of clayey soil as core materials is calculated with the following formula [6]:

$$G_{\max} = 3270\frac{(2.973-e)^2}{1+e}\left(\sigma_0'\right)^{0.5} \tag{6}$$

The Poisson's ratio for core materials is taken as 0.45.

To provide constitutive relations that can better fit the curves of shear modulus degradation and damping ratio increase derived from the experimental tests data, two different modifications are implemented into the FLAC soil model to assess the potential for predicting the seismic behavior and associated deformations. To represent the nonlinear stress-strain behavior of soil more accurately that follows the actual stress-strain path during cyclic loading, the masing behavior is incorporated into FLAC via a FISH subroutine as a first modification. Since, there is a need to accept directly the same degradation curves derived from the test data in fully nonlinear method and to model the correct physics, the second modification is related to incorporate such cyclic data into a hysteretic damping model for FLAC. Modulus degradation curves imply a nonlinear stress-strain curve. Shear modulus and damping of soils are strain dependent. Shear modulus decreases with increasing shear strain and damping increases with increasing strain. In this study, the shear modulus degradation and Damping ratio increase curves for sandy soils proposed by Seed and Idriss [7] and for clayey soils proposed by Vucetic and Dobry [8] are adopted as a reference. Geotechnical properties used in the analyses are presented in Table 1 for the earth dam materials.

Kuhlemeyer and Lysmer [9] showed that for an accurate representation of the wave transmission through the soil model, the spatial element size must be smaller than approximately one-tenth to one-eighth of the wavelength associated with the highest frequency component of the input wave i.e.,

$$\Delta L = \lambda/9 \tag{7}$$

where, λ is the wave length associated with the highest frequency component that contains appreciable energy. Considering above criteria, element size is defined small enough to allow seismic wave propagation throughout the analysis. Rayleigh damping R_d =5% is used in the analyses to compensate for the energy dissipation through the medium [4]. The natural frequency of the dam is determined by a Fourier analysis of the free response of the dam (Figure 3). It shows a fundamental frequency f_1 = 1.71 *Hz* for the dam with height of 40 *m*. The fundamental frequencies of dams with different heights are summarized in Table 2.

Table 1- Geotechnical soil properties

Region	γ_{wet} (kN/m^3)	γ_{sat} (kN/m^3)	υ	Porosity (n)	C (kPa)	Φ degree	K (cm/s)
Core	20	20.5	0.45	0.41	80	8	10^{-7}
Shell	22	23	0.30	0.33	-	40	10^{-2}

Table 2- Fundamental frequency

Frequency (Hz)	Dam Height (m)				
	40	80	120	200	280
f_1	1.7	0.88	0.60	0.36	0.26

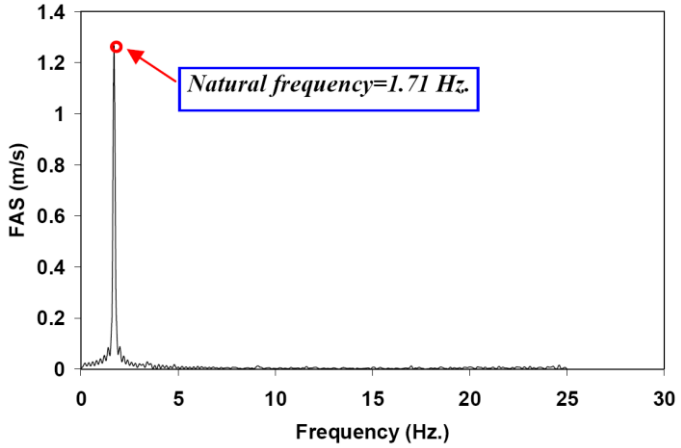

Figure 3. Fourier amplitude spectrum of free horizontal motion at the dam crest

In this paper, three different real acceleration time histories including Tabas (PGA=0.93g in MCE level), Naghan (PGA=0.72g in MDE level) and San Fernando (PGA=0.21g in DBE level) are selected from a database of earthquake records [10]. In the dynamic analyses of dams, the scaled records have been filtered to a maximum frequency of 10 *Hz*, transferred to the "inside" bedrock formation through a standard de-convolution analysis and applied at the base of the numerical model. Pertinent information on the earthquake records are summarized in Table 3, and the corresponding acceleration time histories and Fourier amplitude spectra are depicted in Figure 4.

In the nonlinear analysis which is used in this investigation, the nonlinear stress-strain relationship is followed directly by each element. The damping ratio and shear modulus of the materials at different strain levels are calculated automatically. The real behavior of soils is nonlinear and hysteretic under cyclic loading. This behavior can be simulated by the Masing model [11], which is capable of modeling the dynamic behavior of soils. The shear behavior of the soil, in this model, may be explained by a backbone curve:

$$F_{bb}(\gamma) = \frac{G_{\max}\gamma}{1+\left(G_{\max}/\tau_{\max}\right)|\gamma|} \tag{8}$$

where, $F_{bb}(\gamma)$ is the backbone function, γ is the shear strain amplitude, G_{max} is the initial shear modulus and τ_{max} is the maximum shear stress amplitude.

Table 3- Earthquake records data

Earthquake	Station	Date	M	Closest Distance (km)	PGA (g)	PGV (cm/s)	PGD (cm)
Tabas	Tabas	1978	7.4	94	0.93	121.4	94.58
Naghan	Naghan	1977	5.4	75	0.72	46.20	61.00
San Fernando	Pasadena	1971	6.6	19	0.21	10.90	2.320

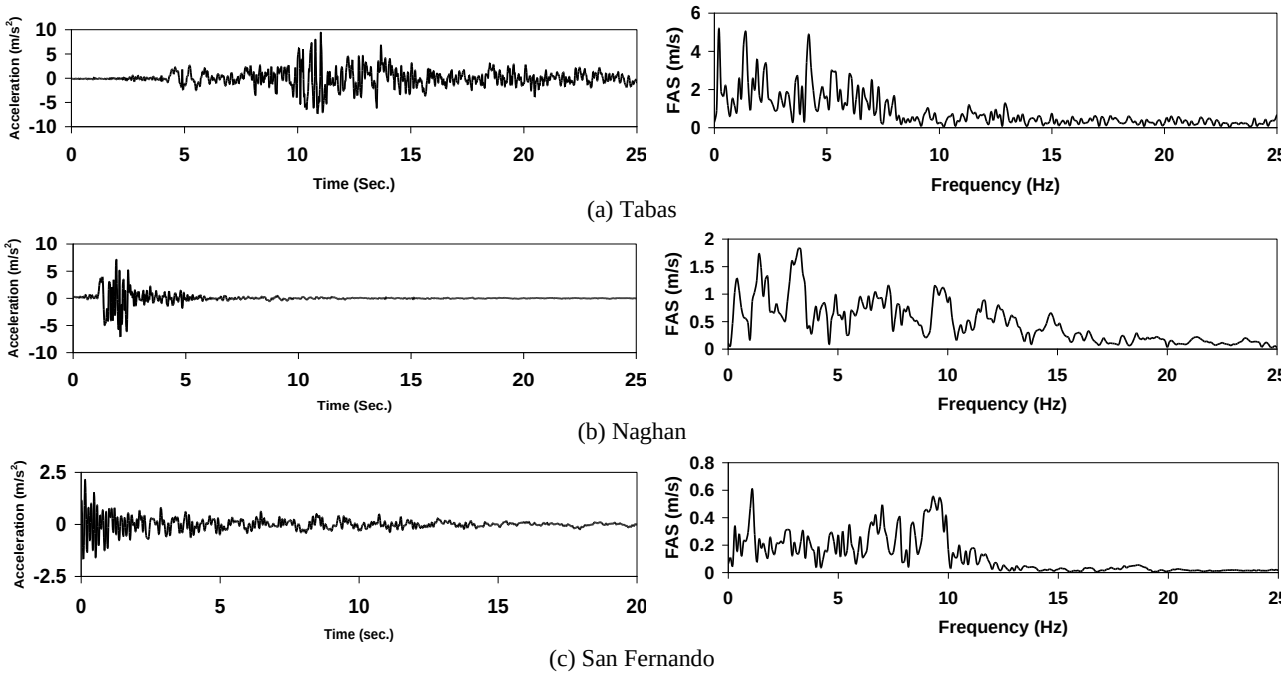

Figure 4. Input acceleration time histories and Fourier amplitude spectra

The stress-strain curve follows the backbone curve in the first loading, but to explain the unloading-reloading, the above equation has to be modified. If the stress returns from point (τ_r, γ_r), the stress-strain curve follows the path below:

$$\frac{\tau-\tau_r}{2}=F_{bb}\left[\frac{\gamma-\gamma_r}{2}\right] \tag{9}$$

In other words, the unloading-reloading curves have the same shape as the backbone curve except the fact that its origin is displaced towards the stress returning point and they have been magnified by a factor of 2 (Figure 5). The Masing rules seem not to be enough to precisely explain the soil response under general cyclic loading. Finn et al. (1977) developed modified rules to describe the irregular loading [12]. They suggested that unloading and reloading curves follow the two rules; If the new unloading or reloading curve exceeds the last maximum strain and cut the backbone curve, it will follow the backbone curve till it reached the next returning point. If a new unloading or reloading curve passes through the previous unloading or reloading curve, it will follow the former stress-strain curve. According to this model, the tangent shear modulus can be defined as below at a point on the backbone curve:

$$G_t=G_{\max}\Big/\left[1+\frac{G_{\max}|\gamma|}{\tau_{\max}}\right]^2 \tag{10}$$

The tangent shear modulus, at a point on the new reloading-unloading curve can be also defined by the following equation:

$$G_t=G_{\max}\Big/\left[1+\frac{G_{\max}}{2\tau_{\max}}|\gamma-\gamma_r|\right]^2 \tag{11}$$

Based on research results, as the number of load cycles increase, the shear stress decreases; that means the shear stress-strain curves get more inclined. To simulate the nonlinear shear stress-strain relationship in this study, the Masing rules have been implemented into FLAC via a series of FISH functions.

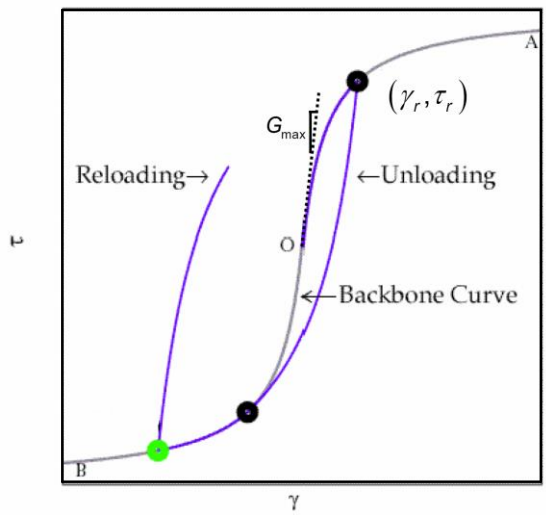

Figure 5. General pattern of loading and unloading of soils

3. VALIDATION ANALYSES

To validate the implementation of the Masing rules in FLAC program, the simulation of one-zone sample with the implemented rules is conducted by using a unit cell as shown in Figure 6 (a). The one-zone sample is modeled with FLAC which consists of a sandy soil and a periodic motion is exerted at its base. Vertical loading is established by gravity only. Equilibrium stresses are installed in soil. The stress-strain loops of the one-zone sample for several cycles are shown in Figure 6(b). It can be observed that shear modulus decreases with increasing shear strain. The hysteretic model seems to handle multiple nested loops in a reasonable manner. There is clearly energy dissipation and shear stiffness degradation during dynamic loading.

To evaluate the applicability of the proposed model, the results obtained from numerical analyses are compared with the experimental counterparts. One of the centrifuge tests related to the embankment performed in VELACS project (VErification of Liquefaction Analysis using Centrifuge Studies [13,14]) is chosen to calibrate the constructed numerical model in FLAC and also consider the ability of the constitutive model in predicting the dynamic response of the dam during seismic loading. It is attempted to create almost similar conditions between laboratory model test and numerical model. The model test configuration is depicted in Figure 7(a). The numerical model constructed in FLAC is shown in Figure 7(b). The numerical results are presented and compared to those of centrifuge test data. Comparisons between the computed and measured results (computed: numerical and Measured: centrifuge test results) are made in Figure 8. The comparisons show that the reference numerical model can predict the dynamic behavior of the earth dam in terms of acceleration and displacement in a rational way.

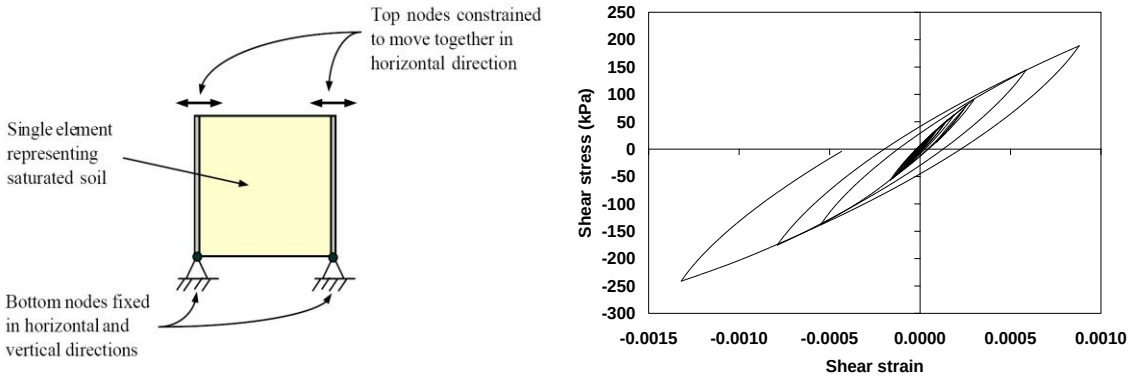

(a) (b)

Figure 6. Simulation of cyclic simple shear test of one-zone sample in FLAC: (a) applied boundary conditions, and (b) Hyteresis loops

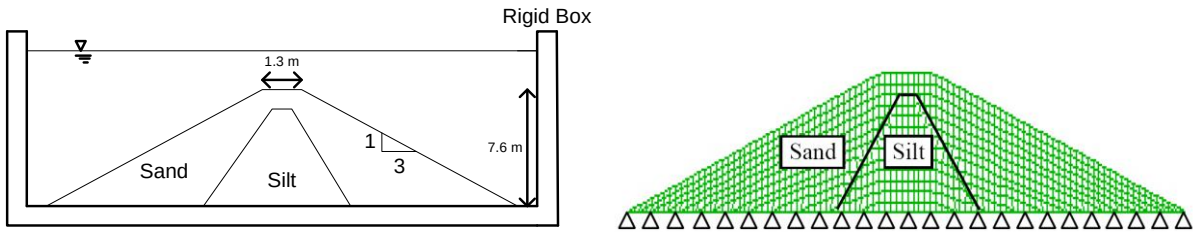

(a) (b)

Figure 7. Model configuration in rigid container: (a) centrifuge test, and (b) numerical grid constructed in FLAC

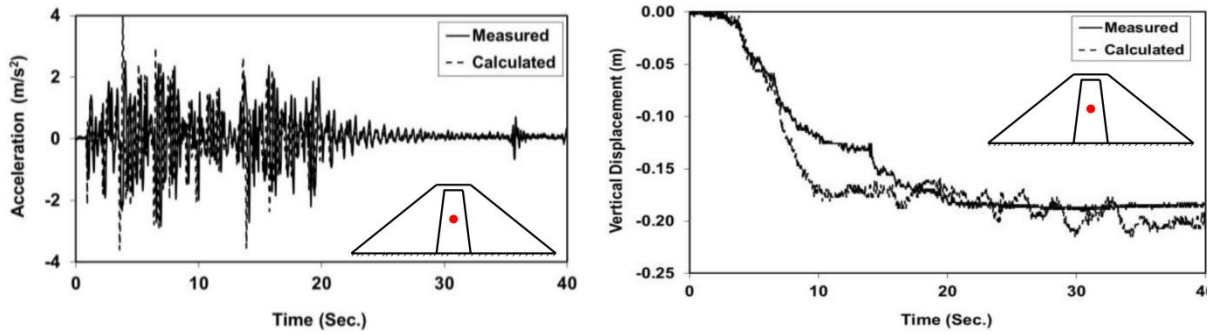

(a) (b)

Figure 8. Measured versus calculated results of centrifuge modeling: (a) acceleration, and (b) displacement time histories at the middle of dam height

The last verification of the proposed numerical model is performed through a real well-documented case history in order to show the ability of the model in simulating the seismic behavior of earth dam during a real earthquake. To this end, the results of non-linear seismic analyses of the Long Valley (LV) earth dam in California subjected to the 1980 Mammoth Lake earthquake are presented and compared with the real measurements recorded at the site [15]. Herein, the results of the previous investigations in the literature have been also presented for comparison purposes. The details information about LV dam can be found in [15]. The LV dam is located in the Mammoth Lake area (California) in the close proximity of active faults. The dam is a rolled earth-fill with an impervious zone that forms the major portion of it. The dam has a maximum height of 55 *m*, a length of 182 *m* at the crest, and upstream and downstream slopes of 3h/1v. The LV dam was instrumented in the 1970's with a multiple-input-output array consisting of 3 accelerometer stations to monitor the boundary conditions and 5 stations to record the dam response (Figure 9). Thus, the array comprised a total of 22 accelerometers linked to a common triggering mechanism. LV dam cross section is shown in Figure 10(a). The numerical model constructed in FLAC is presented in Figure 10(b). In May 1980, a series of 6 earthquakes occurred in the Mammoth Lakes area. The magnitudes of these earthquakes were ranged from M_L = 4.9 to M_L = 6.7, and the induced peak accelerations at the crest center reached 0.5g in the upstream-downstream direction (x direction, Figure 9) during the strongest event. An extensive array of 22 input-output (excitation-response) accelerations was recorded, providing a valuable source of information on the dam seismic response over a wide range of deformation levels. In this study, the LV dam is subjected to the input motion recorded downstream at the outlet during Mammoth Lake earthquakes. The first 12 seconds of the recorded acceleration is used with data point at 0.02 second intervals and peak acceleration equal to 0.135g in the upstream-downstream direction and 0.084g in the vertical direction. The input accelerations are applied in the horizontal and vertical directions of the model base. Of particular interest is the computed acceleration at the crest which can be compared directly with the measured ones. Previous analyses of the LV dam have been reported by Griffiths and Prevost [15], Lai and Seed [16], Yiagos and Prevost [17], Woodward and Griffiths [18]. The first natural frequency obtained from the current study is presented in Table 4 and compared with the other solutions available in literature. The present study gives reasonably close agreement with the other numerical investigations. The crest acceleration responses of the LV dam are computed and compared with the motions recorded at the site in the both time and frequency domains.

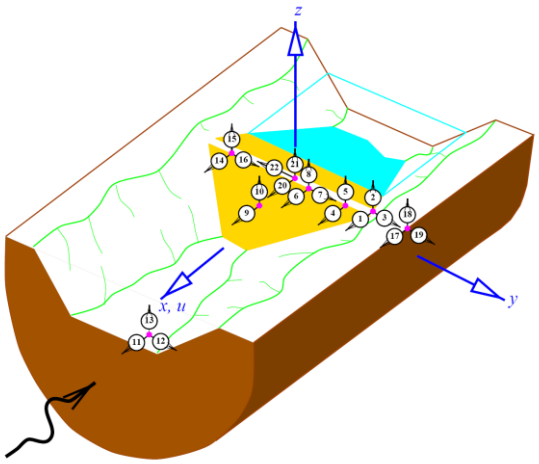

Figure 9. A schematic view of Long Valley canyon and earth dam, and installed instrumentation array [15]

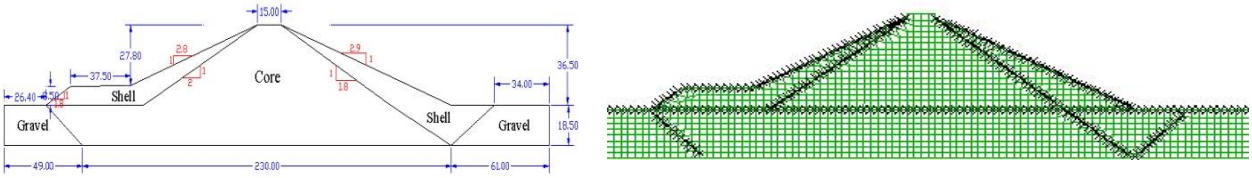

(a) (b)

Figure 10. Long Valley earth dam cross section: (a) dimensions in meter, and (b) numerical grid for seismic analysis

Table 4- First natural frequency of LV dam

Mode	Spectral Analysis	2D FE Analysis	3D FE Analysis	Elasto-plastic FE Analysis	Elasto-plastic FE Analysis	Present Study
	Griffith & Prevost	Griffith & Prevost	Griffith & Prevost	Yiagos & Prevost	Woodward & Griffiths	
	Ref. No. [15]	Ref. No. [15]	Ref. No. [15]	Ref. No. [17]	Ref. No. [18]	
1	1.85	1.76	1.95	1.987	1.79	**1.71**

Figure 11(a) shows the computed horizontal acceleration of the crest. The peak amplitude at the crest has a magnification factor of about 5.47 over the peak base amplitude. The computed response of the crest in the horizontal direction is compared with the measured ones in Figure 11(b). The computed response is plotted with a dashed line. Excellent overall agreement is achieved, with the computed values giving somewhat higher amplitudes. The frequency content of the two time records is compared in the form of a Fourier amplitude spectrum (FAS) in Figure 11(c). The peaks are in close agreement although the computed values show rather more energy associated with the fundamental frequency around 1.8 *Hz*. The frequency content of the up/down stream motion presented in Figure 11(c) shows that the energy is concentrated at a frequency of just under 2 *Hz*.

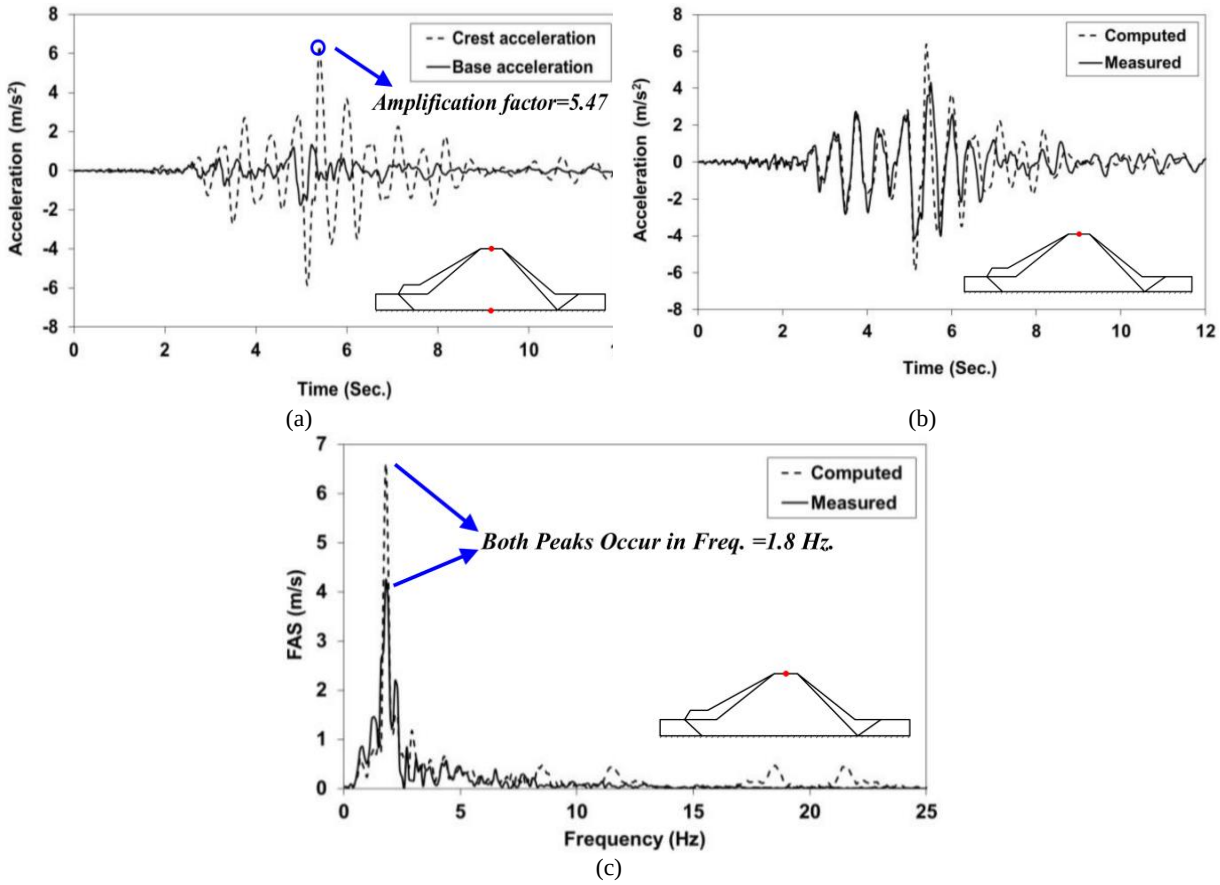

Figure 11. Comparison between computed and measured values of LV dam in horizontal direction at: (a) crest and base, (b) crest acceleration time histories, and (c) Fourier amplitude spectrums

The calculated acceleration in the vertical direction shows less agreement with the measured values. This excitation is noisier than that of horizontal direction and is less intensive. The maximum recorded vertical acceleration at the crest is 0.172g compared with 0.64g in the horizontal direction. The computed accelerations in the vertical direction are compared with the measured ones in Figure 12. The computed values show generally lower amplitudes than the measured ones. The Fourier amplitude spectrum of these time histories is given in Figure 12(c) and the measured values indicate a broad band of frequencies with no particular frequency dominating the situation. The computed values also contain a broad band of frequencies, but with clear peaks in the ranges 2-3 *Hz* and 5-6 *Hz*. The frequency content of the vertical acceleration in the form of Fourier response spectra indicates that the computed values do not reproduce the higher frequencies present in the broad band of measured frequencies. It is noticed that the time and frequency-domain results give good agreement and high correlation in the horizontal direction than those of the vertical direction.

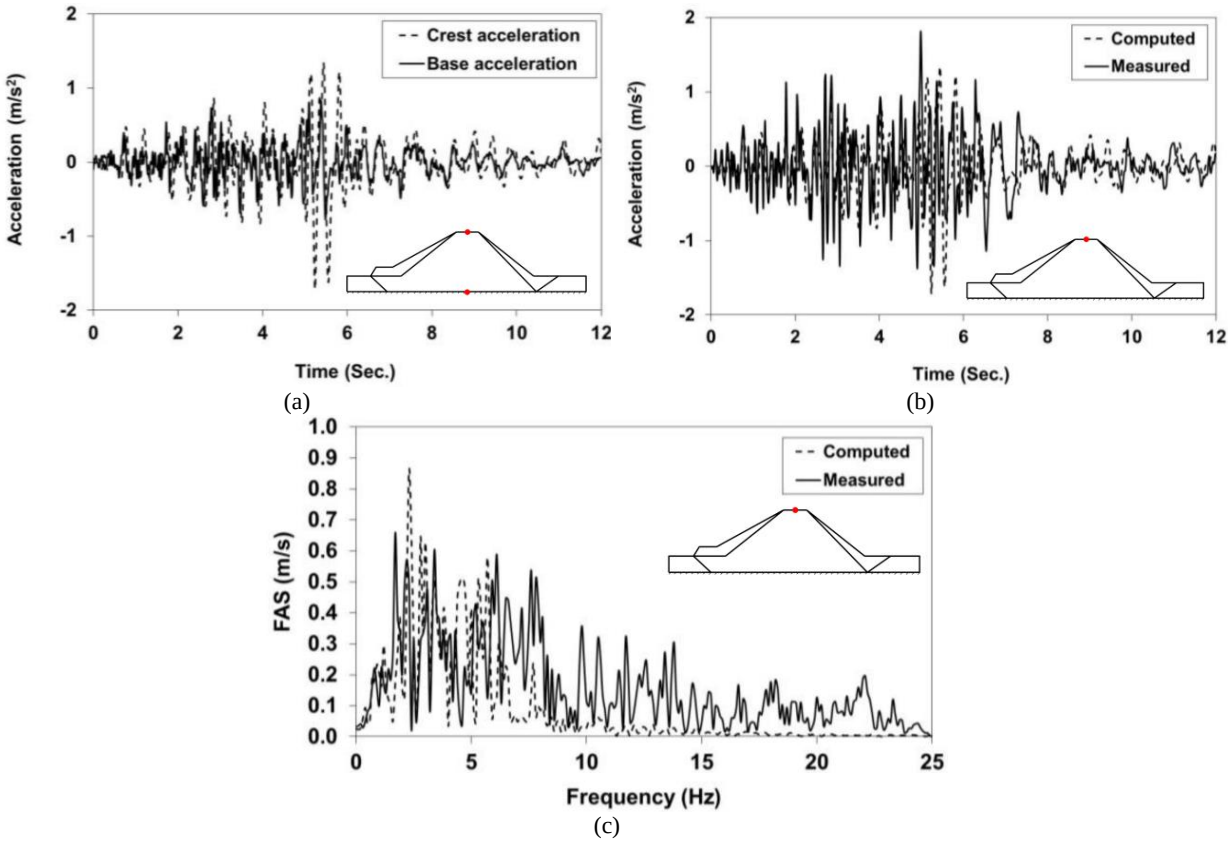

Figure 12. Comparison between computed and measured values of LV dam in vertical direction at: (a) crest and base, (b) crest acceleration time histories, and (c) Fourier amplitude spectrums

The results obtained from validation analysis of the LV dam in term of crest acceleration are compared with those of other previous numerical results available in the literature and summarized in Table 5. These Comparisons show that the current numerical procedure can capture the essential fundamental aspects of the seismic behavior of earth dams very well. It can be concluded that due to the satisfactory modeling of the validation cases, the numerical model is then employed to perform a parametric study on the hypothetical earth dam, as described earlier.

4. NUMERICAL RESULTS AND DISCUSSIONS

Numerous analyses are carried out to investigate the effects dam height and input motion characteristics on the seismic behavior of earth dams. The effects of different types of earthquake on the horizontal deformations at the crest of dams with different heights are shown in Figure 13(a). Besides the displacements, the relevant shear strains are also presented in Figure 13(b). It is clear that the shear strain variation is similar to that of displacement. The horizontal displacements and shear strains in the dam body are increased with increasing dam height. The calculated quantities are much higher for Tabas earthquake and failure occurs in the dam body. Figure 13(a) shows that the computed maximum horizontal displacement at the dam crest is about 94 cm at the end of Tabas earthquake. It can be observed that an increase in the input motion energy leads to a significant increase in the displacements and shear strains. Figure 13(c) illustrates the coupled effects of the dam height and the type of earthquake on the induced maximum acceleration at the dam crest. It is noticed that the crest acceleration is reduced when the dam height increases and no amplification is observed. The reason may be attributed to more flexible behavior, higher damping ratio and larger plastic zones which observed in higher dams. Thus, there is more energy absorption in higher dams with respect to smaller dams due to these factors. It can be seen that the reduction of accelerations in dam crest is more pronounced for the higher dam comparing with the smaller ones.

Table 5- Comparison between numerical studies of LV dam

	Yiagos & Prevost	Woodward & Griffiths	Present Study	Measured values
	Ref. No. [17]	Ref. No. [18]		
Maximum horizontal Acceleration (m/s^2)	0.53g	0.80g	0.61g	0.40g
Minimum horizontal Acceleration (m/s^2)	-0.65g	-0.68g	-0.50g	-0.50g

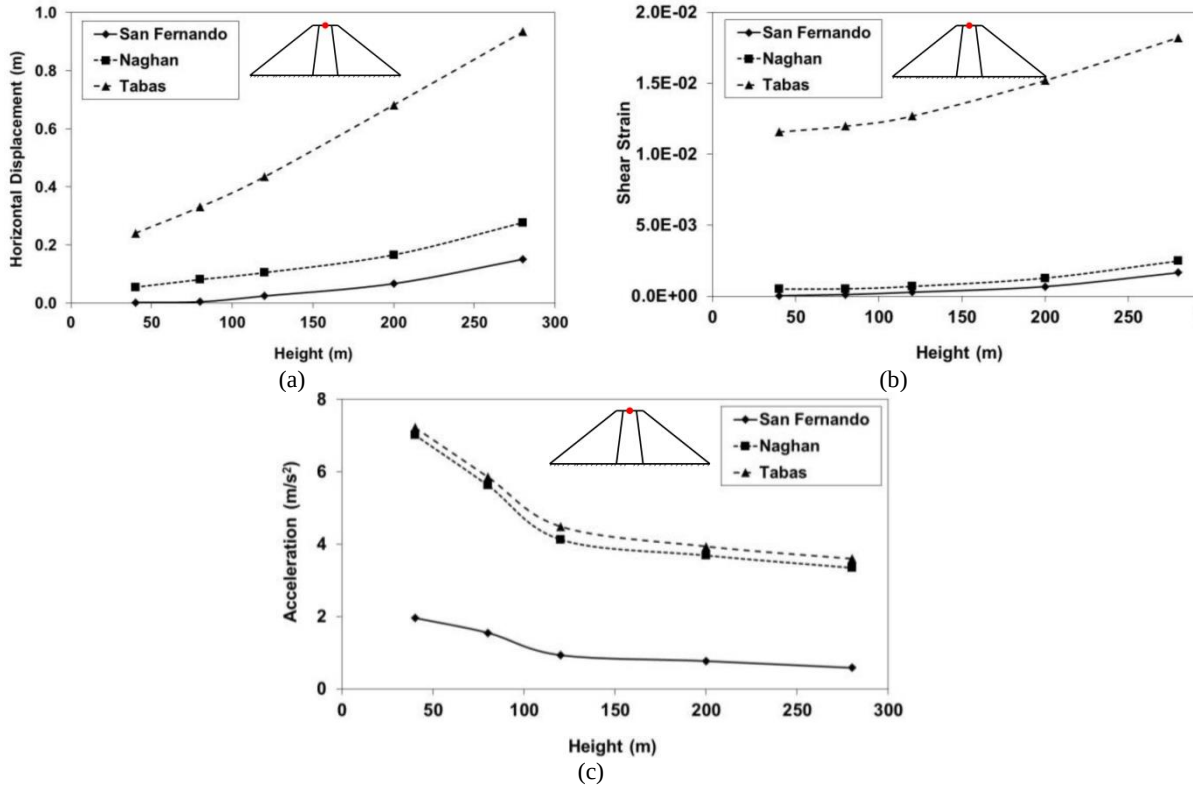

Figure 13. Effect of dam height and input motion characteristics: (a) permanent horizontal displacements, (b) permanent shear strains, and (c) induced maximum accelerations at the dam crest versus dam height for different earthquakes

The pattern of failure mechanism with permanent shear strain contour in the dam body is shown in Figure 14 for two different heights at the end of Naghan earthquake. It is seen that failure occurs in higher dam (280 *m*) comparing with the smaller one (120 *m*). The slip surface in 280 *m* dam is much deeper and clearer than in 120 *m*. It is noteworthy that the PGA of Naghan earthquake (0.72g) is much higher than San Fernando earthquake (0.21g) but the created displacements and shear strains in dam crest due to Naghan earthquake is close to those obtained from San Fernando input motion. It can be concluded that the PGA is not a sufficient parameter for considering the potential of a particular earthquake on the permanent deformations and the other earthquake parameters such as effective duration, intensity, magnitude, frequency content should be taken into account.

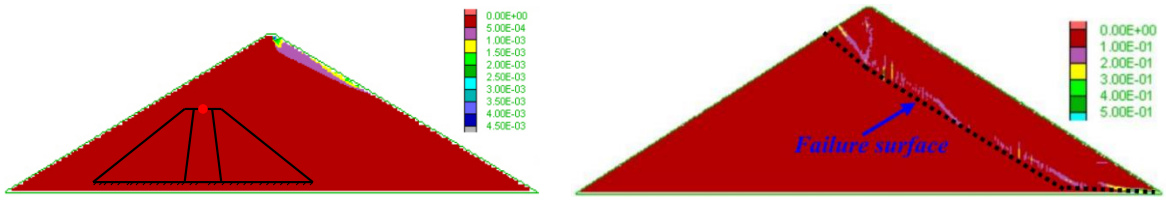

Figure 14. Pattern of failure mechanism in dam body at the end of Naghan earthquake: (a) dam height=120 *m*, (b) dam height=280 *m*

5. CONCLUSIONS

This paper presents the nonlinear seismic analyses of earth dams using finite difference method. An elastic perfectly plastic constitutive model with Mohr-Coulomb failure criterion is used to describe the stress-strain response of the soil. Rayleigh damping is utilized to increase the level of hysteretic damping. The Masing rules are implemented into the constitutive relations to precisely explain the nonlinear soil response under general cyclic loading. The numerical model is comprehensively calibrated against the centrifuge test data as well as the field measurements of a real case history both in the time and frequency domains. The numerical analysis is shown to reproduce well the overall behavior of the dam under the earthquake loading qualitatively as well as quantitatively. After validation, a parametric study has been performed to evaluate the influence of real earthquake loading and dam height on the seismic response of the earth dams. Particular attention is given to the influence of dam height on the dynamic seismic of dam. If the dam materials keep their elastic behavior, then the horizontal acceleration becomes larger along the dam height (from the base to the top). In this case, the higher dams show larger amplification, especially if the natural period of dam body coincides to the periodical nature of earthquake motions. As the dam body behaves as a non-linear or even plastic material when a strong earthquake influences the dam, the attenuation of waves becomes more effective, and consequently the earthquake accelerations descend in magnitude when passing from the base towards to the top. Nonlinear elasto-plastic analyses show that the strongest seismic loading (Tabas earthquake) induces plasticity in a large part of dam body when the height of the dam increases. In fact, the stronger earthquakes are more effective to change the material behavior from elastic to plastic in comparison with the rather weak earthquakes. The higher dams are more flexible than the smaller ones, as a result it affects the shear strains which influence the shear modulus and the attenuating coefficient, and all these effects are on the trend of weakening the accelerations along the height. When the dam is subjected to the earthquake with lower energy, the dam body behaves as an elastic material and thus the induced seismic accelerations inside the dam body become larger from the base to the top. In this case, small plasticity zones are developed in the dam body and then the dam remains safe during earthquake loading.

6. ACKNOWLEDGMENT

The first author wants to express his sincere gratitude to the Iran's National Elites Foundation (INEF) for his moral support and encouragement.

7. REFERENCES

1. Seed, H.B., Lee, K.L., Idriss, I.M. and Makdisi, F.I. (1975), "*The Slides in the San Fernando Dams during the Earthquake of February 9, 1971*", J Geotech Eng Div, ASCE, Vol. 101(GT7), pp. 651–88.
2. Sherard, J.L. (1967), "*Earthquake Considerations in Earth Dam Design*", J. Soil Mech. Found. Div. – ASCE, Vol. 93, pp. 377–401.
3. Ambraseys, N.N. (1960), "T*he Seismic Stability of Earth Dams*", In: Proc. of the Second World Conference on Earthquake Engineering, Tokyo, Japan, pp. 1345–63.
4. Itasca, (2002), "*FLAC User's Guide, Version 4.0*", Itasca Consulting Group. Inc, Minnesota, USA.
5. Kokusho, T. and Esashi, Y. (1981), "*Cyclic Tri-axial Test on Sands and Coarse Material*", In: Proceedings of 10th International Conference on Soil Mechanics and Foundation Engineering, 1981, (Quoted by Ishihara 1986).
6. Hardin, B.O. and Black, W.L. (1968), "*Vibration Modulus of Normally Consolidated Clay*", J. Soil Mechanics & Foundation Engineering, ASCE, 84(2), pp. 1531-1537.
7. Seed, H.B., Wong, R.T., Idriss, I.M., Tokimatsu, K. (1986), "*Moduli and Damping Factors for Dynamic Analyses of Cohesionless Soils*", J. Geotech. Engrg., ASCE, 112 (11), pp. 1016-1032.
8. Vucetic, M. and Dobry, R. (1991), "*Effects of the Soil Plasticity on Cyclic Response*", J. Geotech. Engng ASCE, 117, pp. 89–107.
9. Kuhlmeyer, R.L. and Lysmer, J. (1973), "*Finite Element Method Accuracy for Wave Propagation Problems*", Journal of the Soil mechanics and Foundation Division, ASCE, 99(SM5), pp. 421-427.
10. www.nisee.berkeley.edu
11. Masing, G. (1926), "*Eigenspannungen und Verfestigung beim Messing*", Proc. 2nd Int. Congress on Applied Mechanics, Zurich.
12. Finn, W.D.L., Lee, K.W. and Martin, G.R. (1977), "*An Effective Stress Model for Liquefaction*", J. Geotech. Engrg. Div., ASCE, Vol 103 (6), pp. 517-553.
13. Arulanandan, K. and Scott, R.F. (1993), "*Verification of Numerical Procedures for the Analysis of Soil Liquefaction Problems*", Conference Proceedings, Balkema, Rotterdam, Vol. 1.
14. Arulanandan, K. and Scott, R.F. (1994), "*Verification of Numerical Procedures for the Analysis of Soil Liquefaction Problems*", Conference Proceedings, Balkema, Rotterdam, Vol. 2.
15. Griffith, D.V. and Prevost, J.H. (1988), "*Two- and Three-dimensional Dynamic Finite Element Analyses of the Long Valley Dam*", Geotechnique Vol. 38, pp. 367-388.
16. Lai, S.S. and Seed, H.B. (1985), "*Dynamic Response of Long Valley Dam in the Mammoth Lake Earthquake Series of May 25-27 1980*", Report No. UCB/EERC-85/12, Earthquake Engineering Research Center.
17. Yiagos, A.N. and Prevost, J.H. (1991), "T*ow-phase Elasto-plastic Sseismic Response of Earth Dams : Applications*", Soil Dynamics and Earthquake Engineering Vol. 10, No. 7, pp. 371-381.
18. Woodward, P.K. and Griffiths, D.V. (1996), "*Non-linear Dynamic Analysis of the Long Valley Dam*", Compute Methods and Advances in Geomechanics Vol. 11, No. 6, pp. 635-644.